Some simple vacuum-polarization phenomenology: $e^+e^- \to$ hadrons; the muonic-atom x-ray discrepancy and $g_\mu - 2$

Stephen L. Adler
National Accelerator Laboratory, Batavia, Illinois 60510
and The Institute for Advanced Study, Princeton, New Jersey 08540
(Received 25 July 1974)

We give a simple phenomenological analysis of hadronic and electronic vacuum-polarization effects. We argue that the derivative of the hadronic vacuum polarization, evaluated in the spacelike region, provides a useful meeting ground for comparing $e^+e^- \to$ hadron annihilation data (assumed to arise from one-photon annihilation) with the predictions of parton models and of asymptotically free field theories. Using dispersion relations to connect the annihilation and spacelike regions, we discuss the implications in the spacelike region of a constant e^+e^- annihilation cross section. In particular, we show that a flat cross section between $t = 25$ and $t = 81$ $(\mathrm{GeV}/c)^2$ would provide strong evidence against a precociously asymptotic "color" triplet model for hadrons. We then turn to a consideration of the apparent discrepancy between observed and calculated muonic-atom x-ray transition energies. Specifically, we analyze the hypothesis of attributing this discrepancy to a deviation of the asymptotic electronic vacuum polarization from its expected value, a possibility which is compatible with all current high-precision tests of quantum electrodynamics. Under the additional technical assumption that the postulated discrepancy in the electronic vacuum-polarization spectral function increases monotonically with t, the hypothesis predicts a *decrease* in the expected value of the muon-magnetic-moment anomaly $a_\mu = \frac{1}{2}(g_\mu - 2)$ of at least -0.96×10^{-7}, which should be detectable in the next round of $g_\mu - 2$ experiments and which is substantially larger than likely uncertainties in the hadronic contribution to a_μ. By contrast, postulating a weakly coupled scalar boson ϕ to explain the muonic-atom discrepancy would imply a (very small) increase in the expected value of a_μ. Both the vacuum-polarization and scalar-boson hypotheses (for $M_\phi \geq 1$ MeV) predict a reduction of order 0.027 eV in the $2p_{1/2} - 2s_{1/2}$ transition energy in $[^4\mathrm{He}, \mu]^+$, an effect which may be observable.

I. INTRODUCTION

A number of recent experiments have brought aspects of vacuum-polarization phenomena to the fore. Most prominent are the measurements by the Cambridge Electron Accelerator (CEA) and the Stanford Linear Accelerator Center–Lawrence Berkeley Laboratory (SLAC–LBL) groups of an unexpectedly large cross section for $e^+e^- \to$ hadrons,[1] which gives the absorptive part of the hadronic vacuum polarization. In another area of physics, measurements of muonic-atom x-ray transition energies, undertaken to probe the asymptotic form of the electronic vacuum polarization, appear to show a persistent deviation from theoretical expectations.[2] Forthcoming high-precision measurements of the muon-magnetic-moment anomaly $g_\mu - 2$ will provide an even more sensitive probe of the asymptotic electronic vacuum polarization, and of the hadronic vacuum polarization as well. We present in this paper simple phenomenological arguments which bear on the interpretation of both the annihilation and the muonic experiments. Although fundamentally different physical issues are at stake in the two classes of experiments, common elements of formalism make it natural to consider them together. In Sec. II we use dispersion relations to determine what the timelike-region e^+e^- annihilation data say about the possibility of precocious asymptotic scaling in the spacelike region of the hadronic vacuum polarization (assuming that the observed data do indeed result from one-photon annihilation). In Sec. III we analyze the muonic experiments, with the aim of distinguishing between the possibilities that the muonic-atom x-ray discrepancies may arise from a discrepancy in the asymptotic electronic vacuum polarization, or from the existence of a weakly coupled light scalar boson. Some technical details are given in the appendixes.

II. ELECTRON-POSITRON ANNIHILATION AND PRECOCIOUS SPACELIKE SCALING

The experimental data for electron-positron annihilation into hadrons are conveniently expressed in terms of the ratio $R(t)$, defined as

$$R(t) = \frac{\sigma(e^+e^- \to \text{hadrons}; t)}{\sigma(e^+e^- \to \mu^+\mu^-; t)}, \tag{1}$$

with

$$\sigma(e^+e^- \to \mu^+\mu^-; t) = \left(1+\frac{2m_\mu^2}{t}\right)\left(1-\frac{4m_\mu^2}{t}\right)^{1/2}\frac{4\pi\alpha^2}{3t}$$

$$\approx \frac{4\pi\alpha^2}{3t} = \frac{87\times10^{-33}\ \text{cm}^2}{t\ [\text{in (GeV}/c)^2]} \qquad (2)$$

and with t the virtual-photon four-momentum squared. In Fig. 1 we have plotted (versus $E=t^{1/2}$) a smooth interpolation through all available experimental data for R in the continuum region (excluding the ρ, ω, and ϕ vector-meson contributions). The CEA and SLAC–LBL data points are indicated,[1] while the portion of the curve below $t=2.5$ is taken from the "eyeball" fit given by Silvestrini.[3] When replotted versus t, the data for $R(t)$ rise approximately linearly, indicating a roughly constant hadronic annihilation cross section of 21×10^{-33} cm^2. Assuming that single-photon annihilation is indeed being measured, this behavior strongly contradicts the asymptotic behavior expected on the basis of parton or of asymptotically free-field-theory models of the hadrons, which predict

$$R\sim C, \quad t\to\infty \qquad (3)$$

with the constants C tabulated in Table I. However, it can always be argued that while precocious asymptotic behavior is expected from the SLAC scaling results in the *spacelike* region, the annihilation reaction involves the timelike region, in which asymptotic predictions may be approached much more slowly. This objection naturally raises the question of determining what the annihilation data tell us about behavior in the spacelike region.

To answer this question we consider the renormalized hadronic vacuum-polarization tensor ($t=q^2$)

$$\Pi^{(H)}_{\mu\nu}(q) = (q_\mu q_\nu - tg_{\mu\nu})\Pi^{(H)}(t), \qquad (4)$$

which obeys the dispersion relation

$$\Pi^{(H)}(t) = t\int_{4m_\pi^2}^{\infty}\frac{du}{u}\frac{(1/\pi)\,\text{Im}\Pi^{(H)}(u)}{u-t}, \qquad (5)$$

and which is related to the electron-positron annihilation cross section into hadrons by

$$\sigma(e^+e^- \to \text{hadrons}; u) = \frac{1}{u}\text{Im}\Pi^{(H)}(u)\times(\text{known constants}). \qquad (6)$$

Rather than using Eq. (5) directly, we consider its first derivative

$$\frac{d}{dt}\Pi^{(H)}(t) = \int_{4m_\pi^2}^{\infty} du\frac{(1/\pi)\,\text{Im}\Pi^{(H)}(u)}{(u-t)^2}, \qquad (7)$$

which on substituting Eq. (6) and using Eqs. (1) and (2) can be rewritten as

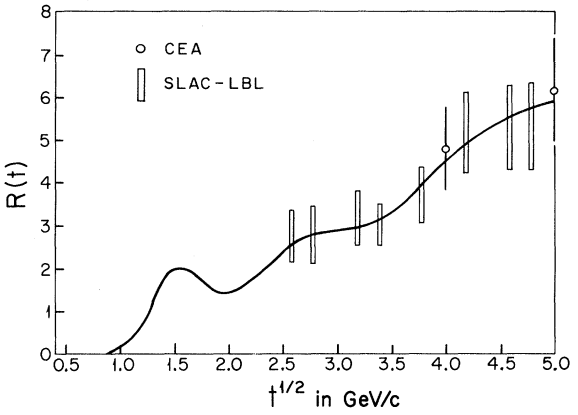

FIG. 1. "Eyeball" fit to the continuum e^+e^- annihilation data. The ρ, ω, and ϕ vector-meson contributions are not included.

$$\frac{d}{dt}\Pi^H(t) = \int_{4m_\pi^2}^{\infty} du\frac{R(u)}{(u-t)^2}\times(\text{known constants}). \qquad (8)$$

Restricting ourselves to the spacelike region $t=-s$, $s>0$ and rescaling to remove the constant factors, we obtain from Eq. (8) our basic relation

$$T(-s) \equiv \int_{4m_\pi^2}^{\infty}\frac{du R(u)}{(s+u)^2} = \frac{d}{dt}\Pi^{(H)}(t)\Big|_{t=-s}\times(\text{known constants}). \qquad (9)$$

The quantity $T(-s)$ has two desirable properties which make it suitable for studying the implications of the annihilation reaction for spacelike-region behavior:

(i) The integrand in Eq. (9) is *positive definite*, and so omitting the high-energy tail of the integral makes an error of known sign. Specifically, if experimental data on R are available only up to a maximum momentum transfer squared t_C, and if we define $T_{\text{obs}}(-s)$ by

$$T_{\text{obs}}(-s) = \int_{4m_\pi^2}^{t_C}\frac{du R(u)}{(s+u)^2}, \qquad (10)$$

TABLE I. Values of C in different models.

Model	C
Simple quark triplet	$\frac{2}{3}$
Color quark triplet	2
Color quark quartet	$\frac{10}{3}$
Han-Nambu triplet	4
Han-Nambu quartet	6

then we have

$$T_{\rm obs}(-s) \leq T(-s), \quad 0 \leq s < \infty. \tag{11}$$

(ii) It is the quantity $T(-s)$ for which parton models and asymptotically free field theories most directly make predictions[4]; the asymptotic predictions for R are always obtained *from* the prediction for $T(-s)$ by a dispersion-relation argument, which is bypassed if we use $T(-s)$ as the primary phenomenological object. In a model in which R asymptotically approaches C, we have

$$T_{\rm th}(-s) \sim C/s, \quad s \to \infty. \tag{12}$$

In asymptotically free field theories, the leading logarithmic correction to Eq. (12) is also determined. Specifically, in the SU(3)⊗SU(3)′ "color" triplet model of the hadrons, one has[4]

$$T_{\rm th}(-s) \sim \frac{2}{s}\left(1+\frac{4}{9}\frac{1}{\ln(s/s_0)}+\cdots\right), \tag{13}$$

with s_0 an arbitrary momentum scale which, in the numerical work, we will take as 2 $(\mathrm{GeV}/c)^2$.

Before proceeding to numerical applications, let us briefly discuss the question of subtractions. Clearly, if the one-photon annihilation cross section were to remain constant as $t \to \infty$, we would have $R(u) \propto u$ as $u \to \infty$ and the integral in Eq. (9) would need an additional subtraction to be well defined.[5] However, such behavior of R would in itself contradict Eq. (3) for all values of C, and hence would rule out all versions of the parton model or of asymptotically free field theories. On the other hand, if Eq. (3) is true for any finite C, then the integral in Eq. (9) converges as it stands and provides a suitable medium for comparing the annihilation data with theoretical expectations in the spacelike region. Note that a constant subtraction term in Eq. (5), which would be present if we renormalize at a point other than $t=0$, would not contribute to the t derivative in Eq. (7); hence the renormalization prescription is not a possible source of ambiguity.

We turn now to the numerical results. In Fig. 2 we plot $T_{\rm obs}(-s)$ [in units where unity = (1 GeV/c)^2], as obtained from all experimental data up to $t_C = 25$ $(\mathrm{GeV}/c)^2$ according to the formula[6]

$$\begin{aligned}
&T_{\rm obs}(-s) = T^{\omega+\phi}(-s) + T^{\rho}(-s) + T^{\rm cont(1)}(-s), \\
&T^{\omega+\phi}(-s) = \frac{9\pi}{\alpha^2}\sum_{V=\omega,\phi}\frac{M_V\Gamma(V\to e^+e^-)}{(s+M_V{}^2)^2}, \\
&T^{\rho}(-s) = \int_{4m_\pi{}^2}^{\infty}\frac{dt}{(s+t)^2}\frac{1}{4}\left(1-\frac{4m_\pi{}^2}{t}\right)^{3/2}|F_\pi(t)|^2, \\
&T^{\rm cont(1)}(-s) = \int_{0.39}^{25}\frac{dt}{(s+t)^2}R(t).
\end{aligned} \tag{14}$$

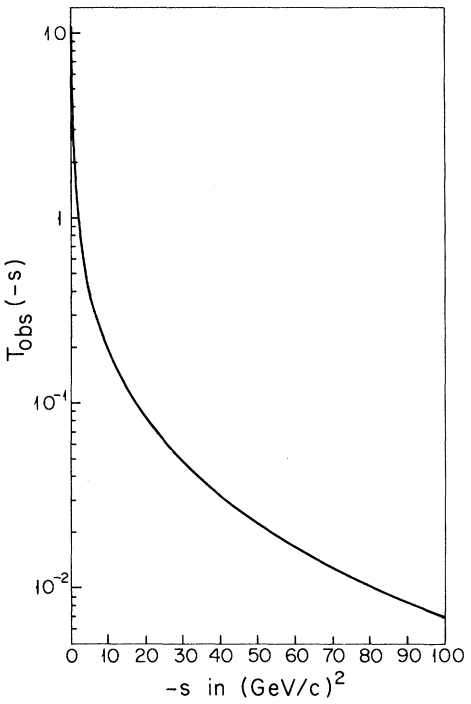

FIG. 2. The function $T_{\rm obs}(-s)$ as obtained from all experimental data up to $t_C = 25$ $(\mathrm{Gev}/c)^2$, in units where unity = (1 GeV/c)^2.

The vector-meson parameters appearing in Eq. (14) are given in Appendix A, while $R(t)$ is the continuum contribution to R graphed in Fig. 1. In Fig. 3 we plot a family of curves, obtained by assuming that for $25 \leq t \leq t_C$ the annihilation cross section $\sigma(e^+e^- \to \text{hadrons}; t)$ remains constant at 21×10^{-33} cm^2. That is, we take

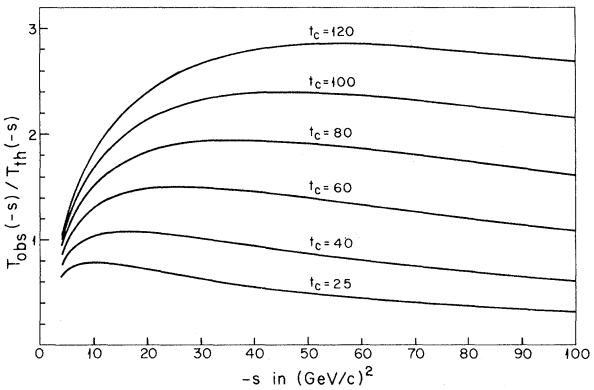

FIG. 3. Ratios of $T_{\rm obs}(-s)$ to $T_{\rm th}(-s)$, with $T_{\rm th}(-s)$ the color-triplet prediction of Eq. (13). The $t_C = 25$ curve uses the presently known data; the curves for higher t_C assume a constant hadronic annihilation cross section of 21×10^{-33} cm^2 above 25 $(\mathrm{GeV}/c)^2$.

$$T_{\rm obs}(-s) = T^{\omega+\phi}(-s) + T^{\rho}(-s) + T^{\rm cont\,(1)}(-s) + T^{\rm cont\,(2)}(-s), \tag{15}$$

$$T^{\rm cont\,(2)}(-s) = \int_{25}^{t_C} \frac{dt}{(s+t)^2} \times 5.94\left(\frac{t}{25}\right) = 0.24\left[\ln\left(\frac{s+t_C}{s+25}\right) - s\,\frac{(t_C-25)}{(s+t_C)(s+25)}\right].$$

Rather than plotting $T_{\rm obs}(-s)$ we have plotted the comparison ratio $T_{\rm obs}(-s)/T_{\rm th}(-s)$, with $T_{\rm th}(-s)$ the "color" triplet prediction of Eq. (13). The $t_C = 25$ curve is just the curve of Fig. 2 divided by Eq. (13); since this curve lies below 1, the existing annihilation data do not yet challenge the "color" triplet model in the spacelike region. (However, since the $t_C = 25$ curve lies well above $\frac{1}{3}$, the existing data already definitively rule out a precociously asymptotic simple quark-triplet model.) Evidently, the curves in Fig. 3 rise rapidly with t_C and show that if the annihilation cross section should remain constant at roughly 21×10^{-33} cm^2 in the region $25 \leq t \leq 81$, which will be accessible at SPEAR II, a precociously asymptotic "color" triplet model would be ruled out in the spacelike region.

To explore the consequences of an annihilation cross section which remains flat up to large t_C, we ignore the vector-meson contributions to $T_{\rm obs}$ and approximate $T^{\rm cont\,(1)}(-s)$ by taking $R(t) \approx 0$, $t < 2$; $R(t) \approx 0.24t$, $2 \leq t \leq 25$, giving the simple analytic expression

$$T_{\rm obs}(-s) = \int_{2}^{t_C} \frac{dt}{(s+t)^2} \times 0.24t = 0.24\left[\ln\left(\frac{s+t_C}{s+2}\right) - s\,\frac{(t_C-2)}{(s+t_C)(s+2)}\right] \approx 0.24\left[\ln\left(\frac{s+t_C}{s}\right) - \frac{t_C}{s+t_C}\right]. \tag{16}$$

Hence,

$$\frac{T_{\rm obs}(-s)}{1/s} \approx R(t_C) f(z), \qquad R(t_C) = 0.24 t_C, \qquad f(z) = \tfrac{1}{2}\ln(1+z) - \frac{1}{1+z}, \quad z = t_C/s. \tag{17}$$

A simple maximization shows that $f(z)$ attains a maximum of 0.22 at $z_M^{-1} = s_M/t_C = 0.46$, and falls to half maximum at $z_L^{-1} = s_L/t_C = 0.053$ and $z_U^{-1} = s_U/t_C = 3.22$. That is, $T_{\rm obs}(-s)/s^{-1}$ reaches a maximum value

$$[T_{\rm obs}(-s)/s^{-1}]^{\rm max} = 0.22\times0.24 t_C = 0.053 t_C, \tag{18a}$$

and lies above half this value in the wide range

$$0.053 t_C \leq s \leq 3.22 t_C. \tag{18b}$$

To give a concrete illustration, if $\sigma(e^+e^- \to \text{hadrons}; t)$ should remain constant up to the maximum t_C of 900 obtainable in a 15 GeV/c on 15 GeV/c storage ring, the maximum of $T_{\rm obs}(-s)/s^{-1}$ would be $0.053\times900 = 48$. This would exclude by a factor of 2 parton or asymptotically free models with $C \leq 24$, thus covering just about every model which has been seriously proposed.

III. MUONIC-ATOM X-RAY DISCREPANCY AND $g_\mu - 2$

Recent studies of the transition energies between large circular orbits in muonic atoms have shown persistent discrepancies between theory and experiment. Because the muonic orbits in question lie well outside the nucleus and well inside the innermost K-shell electrons, one believes that nuclear size and electron screening corrections can be reliably estimated. In particular, the disputed nuclear-size corrections to the vacuum-polarization potential have been reevaluated recently by three independent groups,[7] in good agreement with one another. A survey of all known theoretical corrections has been given by Watson and Sundarasen[2] (see also Rafelski *et al.*[8]), with the conclusion that all important effects within the standard electrodynamic theory have been correctly taken into account. On the experimental side, independent measurements by the groups of Dixit *et al.*[9] and of Walter *et al.*[10] agree on x-ray transition energies which deviate by 2 standard deviations from the theoretical predictions, as summarized in Table II. While it may still turn out that systematic experimental errors or errors or omissions in the theoretical calculations account for the discrepancy, we will assume this not to be the case. Rather, we will treat the discrepancy as a real effect, to be explained by modifications in the conventional theory.

The unique aspect of the muonic-atom transition energies is that, because the muonic orbits lie well inside the electron Compton wavelength, they receive a large contribution from the electronic vacuum-polarization potential and (unlike the more accurate Lamb-shift experiments) they probe the *asymptotic structure* of this potential. Motivated by this observation, our principal focus will be to explore the possibility that the observed x-ray energy discrepancy arises from a nonperturbative deviation of the electronic vacuum polarization from its expected value. Such an effect is qualitatively expected (but with unknown quantitative form) if recent speculations that the fine-

TABLE II. Muonic atom x-ray discrepancies.

Element $_{Z}E$	Transition $^{n}l_{j}\rightarrow{}^{n-1}l-1_{j-1}$	$-\delta E_\gamma \equiv E_\gamma$ (th) $-E_\gamma$ (expt) (eV)	Average discrepancy $-\delta E_\gamma$ (eV)	Reduced average discrepancy $-\delta\bar{E}_\gamma = \dfrac{-\delta E_\gamma}{4.35\ \text{eV}\times Z^2[1/(n-1)^2-1/n^2]}$
$_{20}$Ca	$^3d_{3/2}\rightarrow{}^2p_{1/2}$	7 ± 19	9 ± 13	$(37.2\pm54)\times10^{-3}$
	$^3d_{5/2}\rightarrow{}^2p_{3/2}$	11 ± 17		
$_{22}$Ti	$^3d_{3/2}\rightarrow{}^2p_{1/2}$	-3 ± 19	3.5 ± 13	$(12.0\pm45)\times10^{-3}$
	$^3d_{5/2}\rightarrow{}^2p_{3/2}$	10 ± 18		
$_{26}$Fe	$^3d_{3/2}\rightarrow{}^2p_{1/2}$	21 ± 20	15.5 ± 13	$(37.9\pm32)\times10^{-3}$
	$^3d_{5/2}\rightarrow{}^2p_{3/2}$	10 ± 17		
$_{38}$Sr	$^4f_{5/2}\rightarrow{}^3d_{3/2}$	11 ± 20	5.5 ± 13	$(18.0\pm43)\times10^{-3}$
	$^4f_{7/2}\rightarrow{}^3d_{5/2}$	0 ± 18		
$_{47}$Ag	$^4f_{5/2}\rightarrow{}^3d_{3/2}$	27 ± 20	23 ± 14	$(49.3\pm30)\times10^{-3}$
	$^4f_{7/2}\rightarrow{}^3d_{5/2}$	19 ± 20		
$_{48}$Cd	$^4f_{5/2}\rightarrow{}^3d_{3/2}$	13 ± 19	10 ± 13	$(20.5\pm27)\times10^{-3}$
	$^4f_{7/2}\rightarrow{}^3d_{5/2}$	7 ± 17		
$_{50}$Sn	$^4f_{5/2}\rightarrow{}^3d_{3/2}$	21 ± 21	23 ± 14	$(43.5\pm26)\times10^{-3}$
	$^4f_{7/2}\rightarrow{}^3d_{5/2}$	25 ± 19		
$_{56}$Ba	$^4f_{5/2}\rightarrow{}^3d_{3/2}$	55 ± 23	65.5 ± 15	$(98.8\pm23)\times10^{-3}$
	$^4f_{7/2}\rightarrow{}^3d_{5/2}$	76 ± 20		
	$^5g_{7/2}\rightarrow{}^4f_{5/2}$	12 ± 17	7.5 ± 12	$(24.4\pm39)\times10^{-3}$
	$^5g_{9/2}\rightarrow{}^4f_{7/2}$	3 ± 16		
$_{80}$Hg	$^5g_{7/2}\rightarrow{}^4f_{5/2}$	52 ± 24	45 ± 17	$(71.8\pm27)\times10^{-3}$
	$^5g_{9/2}\rightarrow{}^4f_{7/2}$	38 ± 25		
$_{81}$Tl	$^5g_{7/2}\rightarrow{}^4f_{5/2}$	31 ± 24	35.5 ± 17	$(55.3\pm26)\times10^{-3}$
	$^5g_{9/2}\rightarrow{}^4f_{7/2}$	40 ± 24		
$_{82}$Pb	$^5g_{7/2}\rightarrow{}^4f_{5/2}$	52 ± 21	48.5 ± 14	$(73.7\pm21)\times10^{-3}$
	$^5g_{9/2}\rightarrow{}^4f_{7/2}$	45 ± 18		

structure constant α is electrodynamically determined prove to be correct.[11] We will also briefly consider an alternative explanation which has been advanced to explain the x-ray discrepancy, the possible existence of a weakly coupled light scalar boson.[12]

To calculate the effects of a possible discrepancy in the electronic vacuum polarization we start from the Uehling potential written in spectral form,

$$V(r)=-Z\frac{\alpha^2}{3\pi}\int_{4m_e{}^2}^{\infty}\frac{dt}{t}\left(\frac{e^{-t^{1/2}r}}{r}\right)\rho_e[t],$$

$$\rho_e[t]=\left(1+\frac{2m_e{}^2}{t}\right)\left(1-\frac{4m_e{}^2}{t}\right)^{1/2}. \quad (19)$$

If we now assume that the spectral function $\rho_e[t]$ is changed by nonperturbative effects[13] to $\rho_e[t]+\delta\rho[t]$, then V is replaced by $V+\delta V$, with

$$\delta V(r)=-Z\frac{\alpha^2}{3\pi}\int_{4m_e{}^2}^{\infty}\frac{dt}{t}\left(\frac{e^{-t^{1/2}r}}{r}\right)\delta\rho[t]. \quad (20)$$

This potential contributes to muonic-atom energies through the diagram shown in Fig. 4(a). Since Eq. (20) is a small perturbation and since the muon orbits of interest are appreciably larger in radius than the muon Compton wavelength, in evaluating matrix elements of $\delta V(r)$ we make the approximation of using nonrelativistic hydrogenic muon wave functions. [The same approximation applied to Eq. (19) yields the Uehling energy shifts for all of the levels in Table II to an accuracy of about 5%.[14]] Thus we take

$$R_{n\,n-1}(r)=\left[\left(\frac{2Z}{na_0}\right)^3\frac{1}{(2n)!}\right]^{1/2}e^{-(Z/na_0)r}\left(\frac{2Zr}{na_0}\right)^{n-1},$$

$$a_0=1/\alpha m_\mu, \quad (21)$$

giving for the change in transition energy produced by $\delta V(r)$,

$$\delta E_\gamma=\delta E_n-\delta E_{n-1}$$

$$=\int_0^\infty r^2dr[R_{n\,n-1}(r)^2-R_{n-1\,n-2}(r)^2]\delta V(r). \quad (22)$$

Substituting Eq. (20) into Eq. (22), evaluating the r integral, and using $\alpha^2/(3\pi a_0) = 4.35$ eV, we find

$$\delta\bar{E}_\gamma \equiv \frac{\delta E_\gamma}{4.35\ \text{eV} \times Z^2[1/(n-1)^2 - 1/n^2]}$$

$$= \int_{4m_e{}^2}^{\infty} \frac{dt}{t} f_\gamma[t]\delta\rho[t],$$

$$f_\gamma[t] = [1/(n-1)^2 - 1/n^2]^{-1} \times \left\{ \frac{1}{(n-1)^2}\left[1 + \left(\frac{t}{4m_\mu{}^2}\right)^{1/2} \frac{n-1}{Z\alpha}\right]^{-2(n-1)} - \frac{1}{n^2}\left[1 + \left(\frac{t}{4m_\mu{}^2}\right)^{1/2} \frac{n}{Z\alpha}\right]^{-2n} \right\},$$

$$f_\gamma[0] = 1. \qquad (23)$$

Finally, for convenience in doing the numerical work we make the change of variable

$$t = 4m_e{}^2 e^w, \qquad (24)$$

giving the formulas

$$\delta\bar{E}_\gamma = \int_0^\infty dw\, f_\gamma(w)\delta\rho(w),$$

$$f_\gamma(w) = f_\gamma[4m_e{}^2 e^w], \qquad (25)$$

$$\delta\rho(w) = \delta\rho[4m_e{}^2 e^w].$$

Evidently, in the nonrelativistic approximation which we are using, the shifts in the transition energy δE_γ are j independent, and hence the two transitions for each n, l measure the same weighted integral of $\delta\rho(w)$. Thus, for purposes of comparison with Eq. (25) we average the two discrepancy values for each n, l, as shown in the fourth column of Table II.[15] The "reduced discrepancies" $\delta\bar{E}_\gamma$ introduced in Eq. (23) are tabulated in the final column of Table II.

Before proceeding further with our discussion of the muonic x-ray discrepancy, let us turn to consider another electrodynamic measurement which is sensitive to the asymptotic electronic vacuum polarization, the muon $g_\mu - 2$ experiment. Here the conjectured deviation in the electronic vacuum-polarization spectral function contributes through the diagram of Fig. 4(b). Introducing the standard definition

$$a_\mu = \tfrac{1}{2}(g_\mu - 2) \qquad (26)$$

and using well-known formulas[16] for the photon spectral-function contribution to a, we find that changing the electron vacuum-polarization spectral function induces a $g_\mu - 2$ discrepancy

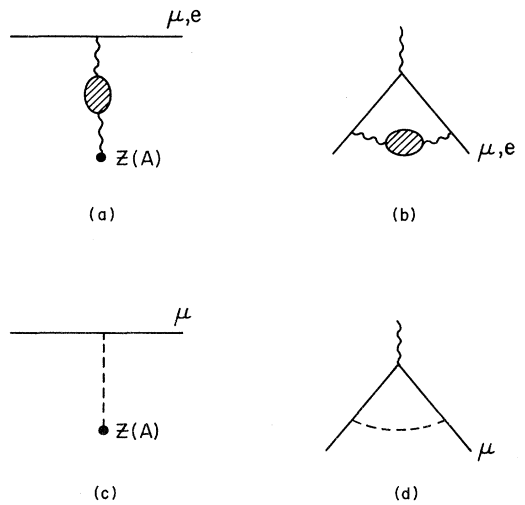

FIG. 4. (a) Diagram by which a vacuum-polarization modification (denoted by the shaded blob) contributes to μ- and e-atomic energy levels. (b) Diagram by which a vacuum-polarization modification contributes to $g_\mu - 2$ and $g_e - 2$. (c) Diagram by which a scalar-meson contributes to μ-atomic energy levels. (d) Diagram by which a scalar meson contributes to $g_\mu - 2$.

$$\delta a_\mu = \frac{\alpha^2}{3\pi^2} \int_{4m_e{}^2}^{\infty} \frac{dt}{t} \frac{1}{2} f_a[t]\delta\rho[t],$$

$$f_a[t] = 2\int_0^1 dx \frac{x^2(1-x)}{x^2 + (1-x)t/m_\mu{}^2}, \quad f_a[0] = 1. \qquad (27)$$

Using $\alpha^2/(3\pi^2) = 1.80 \times 10^{-6}$ and making the change of variable of Eq. (24), we get the convenient formula

$$\delta a_\mu = 1.80 \times 10^{-6} \tfrac{1}{2} \int_0^\infty dw\, f_a(w)\delta\rho(w),$$

$$f_a(w) = f_a[4m_e{}^2 e^w]. \qquad (28)$$

The result of carrying out the integrations in the expression for $f_a(t)$ is given in Appendix B.

Let us now return to our analysis of the muonic x-ray discrepancy. The kernels $f_\gamma(w)$ for four representative transitions are plotted in Fig. 5. Our numerical evaluation shows that the six transitions listed in Table III have weight functions f_γ which are nearly identical (their spread around curve b in Fig. 5 is less than one third of the spacing between curve b and curve a); averaging the weight functions for these transitions gives the function $\bar{f}_\gamma$ plotted in Fig. 6. Substituting the average of the reduced discrepancies for these six transitions into Eq. (25), we find

$$(54.5 \pm 10) \times 10^{-3} = \text{average of six } (-\delta\bar{E}_\gamma) = -\int_0^\infty dw\, \bar{f}_\gamma(w)\delta\rho(w), \qquad (29)$$

indicating that the sign of the discrepancy corresponds to a *reduction* in the electronic vacuum-polarization spectral function from its usual value of Eq. (19). Referring back to Fig. 6, we note that the function f_a is always greater than $\bar{f}_\gamma$. Hence if we assume that $\delta\rho(w)$ is always of negative sign in the region where f_a and $\bar{f}_\gamma$ are nonzero [as might reasonably be expected if we are just entering a new region of physics where the discrepancy $\delta\rho(w)$ is turning on], we learn that

$$\int_0^\infty dw\, f_a(w)\delta\rho(w) \leq -(54.5\pm 10)\times 10^{-3}. \tag{30}$$

Comparing Eq. (30) with Eq. (28) we then get an inequality for the $g_\mu - 2$ discrepancy,

$$\delta\rho \leq 0 \Rightarrow \begin{cases} \delta a_\mu \leq -1.80\times 10^{-6}\tfrac{1}{2}(54.5\pm 10)\times 10^{-3} \\ \quad = -(0.49\pm 0.09)\times 10^{-7}, \\ \delta a_\mu/a_\mu \leq -42\pm 8 \text{ ppm}. \end{cases} \tag{31}$$

A stronger prediction follows if, in addition to our assumption on the sign of $\delta\rho$, we assume that the magnitude of $\delta\rho$ increases monotonically with t (again as might reasonably be expected for an effect just turning on). Then defining

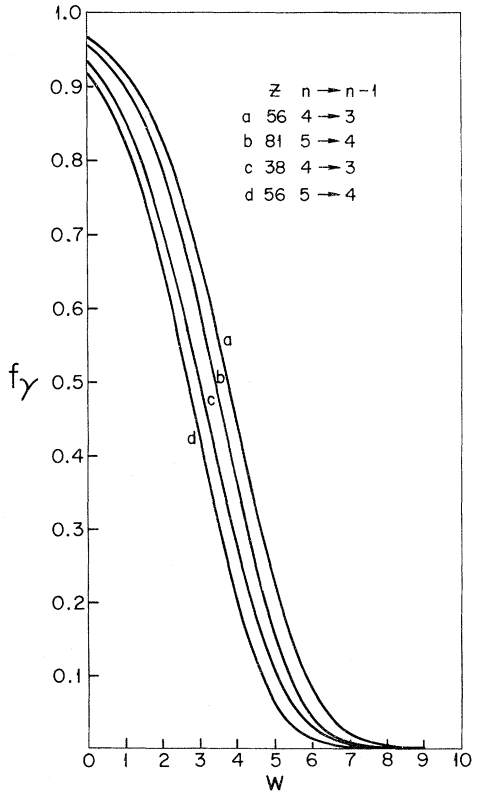

FIG. 5. Kernels f_γ for some representative transitions.

TABLE III. Transitions with nearly identical f_γ.

Element $_zE$	Transition $^nl \to {}^{n-1}l - 1$	Reduced average discrepancy $-\delta\bar{E}_\gamma$
$_{47}$Ag	$^4f \to {}^3d$	$(49.3\pm 30)\times 10^{-3}$
$_{48}$Cd	$^4f \to {}^3d$	$(20.5\pm 27)\times 10^{-3}$
$_{50}$Sn	$^4f \to {}^3d$	$(43.5\pm 26)\times 10^{-3}$
$_{80}$Hg	$^5g \to {}^4f$	$(71.8\pm 27)\times 10^{-3}$
$_{81}$Tl	$^5g \to {}^4f$	$(55.3\pm 26)\times 10^{-3}$
$_{82}$Pb	$^5g \to {}^4f$	$(73.7\pm 21)\times 10^{-3}$
Weighted average of six reduced discrepancies [a]:		$(54.5\pm 10)\times 10^{-3}$

[a] We have treated the errors as if they were purely statistical and have quoted the rms error for the average.

$$\bar{f}_\gamma(w) = 0, \quad w < 0, \tag{32}$$

we find that we can represent $f_a(w)$ as a superposition of displaced curves $\bar{f}_\gamma$,

$$f_a(w) = 1.016\bar{f}_\gamma(w) + \int_0^{10.2} dw'\, c(w')\bar{f}_\gamma(w-w'), \tag{33}$$

with the positive weight function c plotted in Fig. 6. Multiplying by $\delta\rho(w)$ and integrating we get

$$\int_0^\infty dw\, f_a(w)\delta\rho(w) = 1.016\int_0^\infty dw\,\bar{f}_\gamma(w)\delta\rho(w) + \int_0^{10.2} dw'\, c(w') \times \int_0^\infty dw\,\bar{f}_\gamma(w-w')\delta\rho(w). \tag{34}$$

But using Eq. (32) and the assumed monotonicity

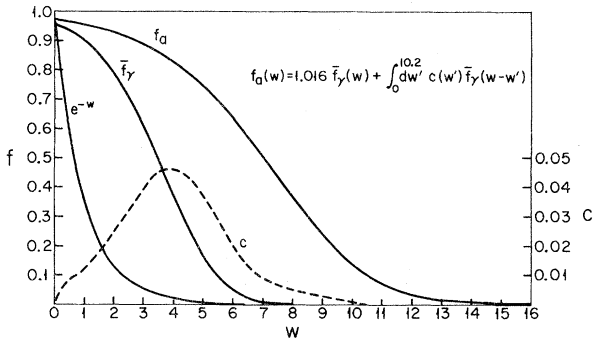

FIG. 6. Plots of the kernels $\bar{f}_\gamma$ and f_a [see the discussion which follows Eqs. (28) and (29) of the text].

of $\delta\rho$, we get

$$\int_0^\infty dw \bar{f}_\gamma(w-w')\delta\rho(w) = \int_0^\infty dw\, \bar{f}_\gamma(w)\delta\rho(w+w') \leq \int_0^\infty dw\, \bar{f}_\gamma(w)\delta\rho(w)\,, \quad (35)$$

and so we learn

$$\int_0^\infty dw f_a(w)\delta\rho(w) \leq \left(1.016 + \int_0^{10.2} dw' c(w')\right) \times \int_0^\infty dw\, \bar{f}_\gamma(w)\delta\rho(w) = 2.00 \times \int_0^\infty dw\, \bar{f}_\gamma(w)\delta\rho(w)\,. \quad (36)$$

Thus adding the assumption of monotonicity doubles the prediction of Eq. (30), giving

$$\left.\begin{matrix}\delta\rho \leq 0 \\ |\delta\rho| \uparrow\end{matrix}\right\} \Rightarrow \begin{cases}\delta a_\mu \leq -(0.98 \pm 0.18)\times 10^{-7} \\ \delta a_\mu / a_\mu \leq -84 \pm 16 \text{ ppm}\,.\end{cases} \quad (37)$$

Equation (37) is the principal result of our analysis.

Two remarks about Eq. (37) are in order. First, the discrepancy in a_μ predicted in Eq. (37) is compatible, within errors, with the present agreement of experiment with the conventional electrodynamic prediction for a_μ,[17]

$$a_\mu(\text{expt}) - a_\mu(\text{conventional QED}) = (2.5 \pm 3.1)\times 10^{-7}\,. \quad (38)$$

However, it should be readily observable in the next $g_\mu - 2$ experiment, where it is anticipated[17] that the current experimental error of $\pm 3.1\times 10^{-7}$ ($=\pm 270$ ppm in $\delta a_\mu / a_\mu$) will be reduced by a factor of 20. Second, the predicted effect is substantially larger than the likely remaining uncertain contributions to a_μ. Specifically, these are the following.

(i) The 8th-order electrodynamic contribution to a_μ, which has been variously estimated[18] as 6×10^{-9}–7×10^{-9}, with an uncertainty of perhaps a few parts in 10^{-9}.

(ii) The uncertainty in the hadronic contribution to a_μ. Including the ρ, ω, and ϕ resonances and integrating the e^+e^- annihilation continuum up to $t_C = 25$ gives a known hadronic contribution of 71×10^{-9} with an estimated uncertainty of $\pm 7\times 10^{-9}$ (see Appendix B). The unknown contribution of the e^+e^- annihilation continuum beyond $t_C = 25$ will of course depend on the behavior of $R(t)$ in that region. To get a crude estimate, let us make the (hopefully extreme) assumption that $R(t)$ rises linearly up to $t = (460)^2$, where the one-photon annihilation cross section violates the $J = 1$ unitarity limit,[19] and cut off the integral at this point. This procedure suggests a bound on the high-energy hadronic contribution to a_μ of 15×10^{-9}. (Again see Appendix B.)

(iii) Unified gauge theories of the weak and electromagnetic interactions which do not have charged heavy leptons typically give contributions[20] to a_μ in the range from a few to ten parts in 10^{-9}. Specifically, the Weinberg-Salam SU(2)⊗U(1) model predicts a contribution to a_μ of less than 9×10^{-9}. Thus, from (i), (ii), and (iii) we conclude that the sum of unknown contributions to a_μ is likely to be no bigger than $\approx 35\times 10^{-9}$, and hence should not mask the effect predicted in Eq. (37).

Although we have shown that the inequality of Eq. (37) does not contradict the current $g_\mu - 2$ experiment, we must still verify that it is possible to find specific functional forms $\delta\rho(w)$ which fit the muonic x-ray discrepancy without seriously violating any of the conventional tests of QED, including the very high precision $g_e - 2$ and Lamb-shift experiments.[21] A postulated vacuum-polarization discrepancy contributes to $g_e - 2$ through the diagram of Fig. 4(b), giving a formula identical to Eq. (27) apart from the replacement of m_μ in $f_a[t]$ by m_e. The smallness of m_e then permits use of the large-t asymptotic expression $\frac{1}{2}f_a \approx m_e^2/(3t)$, giving the simple expression

$$\delta a_e \approx 0.60\times 10^{-6} \int_{4m_e^2}^\infty \frac{dt}{t}\frac{m_e^2}{t}\delta\rho[t] = 0.15\times 10^{-6}\int_0^\infty dw\, e^{-w}\delta\rho(w)\,. \quad (39)$$

Comparing Eq. (39) with the current difference between experiment and theory for a_e,[22]

$$a_e(\text{experiment}) - a_e(\text{conventional QED}) = (5.6 \pm 4.4)\times 10^{-9}\,, \quad (40)$$

we get the restriction

$$\int_0^\infty dw\, e^{-w}\delta\rho(w) = (37 \pm 29)\times 10^{-3}\,. \quad (41)$$

Next we consider the Lamb shift, which receives contributions from a vacuum-polarization discrepancy via the diagram of Fig. 4(a). Working again in the nonrelativistic hydrogenic approximation, we find for the change in the $2s$-$2p$ Lamb-transition energy

$$\delta\mathcal{L} \equiv \delta E_{2s\to 2p}$$
$$= \int_0^\infty r^2 dr [R_{20}(r)^2 - R_{21}(r)^2]\delta V(r)$$
$$= -\frac{a_0\alpha^2}{6\pi}\int_{4m_e{}^2}^\infty \frac{dt\,\delta\rho[t]}{(1+t^{1/2}a_0/Z)^4}. \quad (42)$$

Since $t^{1/2}a_0Z^{-1} = (t^{1/2}/m_e)\alpha^{-1}Z^{-1} \gg 1$, we can neglect the 1 in the denominator of Eq. (42), giving

$$\delta\mathcal{L} = -\frac{Z^4\alpha^5 m_e}{6\pi}\int_{4m_e{}^2}^\infty \frac{dt}{t}\frac{m_e{}^2}{t}\delta\rho[t], \quad (43)$$

which evidently measures the same integral over $\delta\rho$ as does $g_e - 2$. It is easy to see that the formula for the $ns \to np$ Lamb transition is obtained by multiplying Eq. (43) by $(2/n)^3$. Hence, using the fact that

$$\frac{\alpha^5 m_e}{30\pi} \approx 27.1 \text{ MHz}, \quad (44)$$

we get the relation

$$\int_0^\infty dw\, e^{-w}\delta\rho(w)$$
$$= \frac{n^3[\mathcal{L}_{nZ}(\text{conventional QED}) - \mathcal{L}_{nZ}(\text{expt})]}{Z^4 \times 271 \text{ MHz}}. \quad (45)$$

In Table IV we have tabulated the right-hand side of Eq. (45) for a series of measured Lamb transitions.[23] Taking a weighted average of the four best determinations [the two measurements for $H(n=2)$ and the measurements for $D(n=2)$ and $He^+(n=2)$], we find

$$\int_0^\infty dw\, e^{-w}\delta\rho(w) = (0.29 \pm 1.0)\times 10^{-3}, \quad (46)$$

evidently a much tighter restriction than is obtained from $g_e - 2$.

Our procedure for searching for satisfactory functional forms $\delta\rho$ is now as follows. Let

$$\begin{aligned}
&\delta\bar{E}_\gamma(i), \sigma(i) = \text{experimental reduced discrepancies and standard deviations from Table II, } i = 1, \ldots, 12;\\
&F(i) = \text{theoretical fit to reduced discrepancies, } i = 1, \ldots, 12;\\
&\delta a_\mu^{\text{th}} = \text{predicted change in } a_\mu,\\
&\delta I^{\text{th}} = \text{predicted value of } \int_0^\infty dw\, e^{-w}\delta\rho(w).
\end{aligned} \quad (47)$$

We form two χ^2:

$$\chi^2{}_1 \equiv \sum_{i=1}^{12}\left[\frac{F(i) - \delta\bar{E}_\gamma(i)}{\sigma(i)}\right]^2,$$
$$\chi^2{}_2 = \chi^2{}_1 + \left(\frac{\delta a_\mu{}^{\text{th}} - 2.6\times 10^{-7}}{3.1\times 10^{-7}}\right)^2 + \left(\frac{\delta I^{\text{th}} - 37\times 10^{-3}}{29\times 10^{-3}}\right)^2 + \left(\frac{\delta I^{\text{th}} - 0.29\times 10^{-3}}{1.0\times 10^{-3}}\right)^2; \quad (48)$$

the first tests the fit to the muonic x-ray discrepancies alone, while the second tests the combined fit to the x-ray data and the $g_\mu - 2$, $g_e - 2$ and Lamb-shift experiments. For each assumed functional form of $\delta\rho$, we treat the over-all normalization as a free parameter and adjust it to minimize either $\chi^2{}_1$ or $\chi^2{}_2$, corresponding respectively to $12 - 1 = 11$ or $15 - 1 = 14$ degrees of freedom. A sampling of results of this procedure is shown in Tables V and VI. We conclude from these fits the following.[24]

(i) Functional forms giving good $\chi^2{}_2$ fits can be found. When these same functional forms are fit by the $\chi^2{}_1$ procedure the coefficients change by only about 25%, which is satisfactory.

(ii) The forms which give good $\chi^2{}_2$ fits are all nearly step-function-like in character, with a turn-on at $w \approx 2$–3 [i.e., at $t \approx (30$–$80)m_e{}^2$]. The smallness below $w \sim 2$ is required by the Lamb-

TABLE IV. Lamb-shift measurements.

System	Conventional QED (MHz)	Expt (MHz)	Right-hand side of Eq. (41)
$H(n=2)$	1057.911 ± 0.012	1057.90 ± 0.06	$(0.33 \pm 1.80)\times 10^{-3}$
		1057.86 ± 0.06	$(1.50 \pm 1.80)\times 10^{-3}$
$H(n=3)$	314.896 ± 0.003	314.810 ± 0.052	$(8.57 \pm 5.18)\times 10^{-3}$
$H(n=4)$	133.084 ± 0.001	133.18 ± 0.59	$(-22.7 \pm 139)\times 10^{-3}$
$D(n=2)$	1059.271 ± 0.025	1059.28 ± 0.06	$(-0.27 \pm 1.92)\times 10^{-3}$
$He^+(n=2)$	$14\,044.765 \pm 0.613$	$14\,045.4 \pm 1.2$	$(-1.18 \pm 2.49)\times 10^{-3}$
$He^+(n=3)$	4184.42 ± 0.18	4183.17 ± 0.54	$(7.79 \pm 3.55)\times 10^{-3}$
$He^+(n=4)$	1769.088 ± 0.076	1769.4 ± 1.2	$(-4.60 \pm 17.7)\times 10^{-3}$
$Li^{++}(n=2)$	$62\,762 \pm 9$	$62\,765 \pm 21$	$(-1.1 \pm 8.3)\times 10^{-3}$
$C^{5+}(n=2)$	$(783.678 \pm 0.251)\times 10^{-3}$	$(744.0 \pm 7)\times 10^{-3}$	$(904 \pm 159)\times 10^{-3}$

TABLE V. Sample functional forms giving statistically satisfactory fits.

(1) Fits minimizing χ^2_2

Functional form $\delta\rho(w)$	χ^2_2	$10^7\delta a_\mu$	$\delta\mathcal{L}(H)$ (MHz) [a]
$-0.053\theta(w-3)$	12.1	−1.9	0.08
$-0.071\left(\frac{w-3}{w}\right)^{0.2}\theta(w-3)$	12.1	−2.1	0.08
$-0.16\left(\frac{w-2}{w}\right)^{2}\theta(w-2)$	12.9	−2.4	0.08

(2) Fits minimizing χ^2_1

Functional form $\delta\rho(w)$	χ^2_1	$10^7\delta a_\mu$	$\delta\mathcal{L}(H)$ (MHz) [a]
$-0.066\theta(w-3)$	7.9	−2.3	0.10
$-0.088\left(\frac{w-2}{w}\right)^{0.2}\theta(w-3)$	7.9	−2.6	0.10
$-0.21\left(\frac{w-2}{w}\right)^{2}\theta(w-2)$	8.1	−3.1	0.11

(3) Reduced discrepancies predicted by the fit $-0.071[(w-3)/w]^{0.2}\theta(w-3)$

Z	20	22	26	38	47	48	50	56	56	80	81	82
Transition $n\to n-1$	3→2	3→2	3→2	4→3	4→3	4→3	4→3	4→3	5→4	5→4	5→4	5→4
$-10^3\times\delta\bar{E}_\gamma$ (expt)	37.2 ±54	12.0 ±45	37.9 ±32	18.0 ±43	49.3 ±30	20.5 ±27	43.5 ±26	98.8 ±23	24.4 ±39	71.8 ±27	55.3 ±26	73.7 ±21
$-10^3\times\delta\bar{E}_\gamma$ (fit)	40.6	46.2	57.3	30.5	42.5	43.8	46.5	54.2	21.6	40.0	40.8	41.6

[a] See the comment in Ref. 25.

shift data, while the slow growth above the turn-on is needed in order not to violate the current limits on deviations in $g_\mu - 2$.

(iii) All of the good fits satisfy $\delta\rho \lesssim -0.03$ for large w. This is a general feature for any monotonic form $\delta\rho$ which is small in the Lamb-shift region $w \leq 2$, since (using the fact that $\bar{f}_\gamma \approx 0$ for $w \gtrsim 9$) we have

$$\begin{aligned} -54.5\times10^{-3} &= \int_0^\infty dw\,\bar{f}_\gamma(w)\delta\rho(w) \\ &\approx \int_2^9 dw\,\bar{f}_\gamma(w)\delta\rho(w) \\ &\gtrsim \delta\rho(9)\int_2^9 dw\,\bar{f}_\gamma(w) = 1.6\times\delta\rho(9)\,, \end{aligned} \tag{49}$$

that is,

$$-0.034 \gtrsim \delta\rho(9)\,. \tag{50}$$

Possible implications of Eq. (50) for QED tests involving timelike photon vertices will be discussed elsewhere.[25]

One additional place where a vacuum-polarization discrepancy should produce interesting effects is in the Lamb shift in muonic helium.[26] Applying Eq. (42) to this system (and noting that the $2p$ level here lies above the $2s$ level), we find

$$\begin{aligned} \delta\mathcal{L}([^4\mathrm{He},\mu]^+) &\equiv \delta E_{2p\to2s} \\ &= \frac{a_0\alpha^2}{6\pi}\int_{4m_e{}^2}^\infty dt\,\frac{\delta\rho[t]}{(1+t^{1/2}a_0/Z)^4} \\ &= \frac{2}{3\pi}\alpha\frac{m_e{}^2}{m_\mu}\int_0^\infty dw\,f_{\mathrm{He}}(w)\delta\rho(w)\,, \\ f_{\mathrm{He}}(w) &= \frac{e^w}{[1+(m_e/m_\mu\alpha)e^{w/2}]^4}\,, \quad f_{\mathrm{He}}(0)\approx0.13\,. \end{aligned} \tag{51}$$

TABLE VI. Results of step-function fits.

Functional form $\delta\rho$	χ^2_2	$10^7\delta a_\mu$	$\delta\mathcal{L}(H)$ (MHz) [a]
$-0.004\theta(w-0.5)$	38	−0.23	0.08
$-0.014\theta(w-1.5)$	21	−0.69	0.10
$-0.032\theta(w-2.5)$	14	−1.3	0.09
$-0.072\theta(w-3.5)$	12	−2.3	0.07
$-0.16\theta(w-4.5)$	13	−4.0	0.06
$-0.37\theta(w-5.5)$	22	−6.7	0.05
$-0.39\theta(w-6.5)$	43	−5.0	0.02

[a] See the comment in Ref. 25.

Numerical evaluation of Eq. (51) shows that $f_{\mathrm{He}}(w)/0.13$ lies within 20% of $\bar{f}_\gamma(w)$ in the range $0 \leq w \leq 6$ where neither is vanishingly small. Hence independent of the detailed form of $\delta\rho$, we find the prediction

$$\delta\mathcal{L}([^4\mathrm{He}, \mu]^+) \sim \frac{2}{3\pi}\alpha\frac{m_e{}^2}{m_\mu} \times (-54.5\times 10^{-3})\times 0.13 \approx -0.027 \text{ eV}, \quad (52)$$

which may be an observable effect.

At this point let us conclude our examination of vacuum-polarization effects and turn to an alternative explanation for the muonic x-ray discrepancy, the possible existence[12] of a weakly coupled scalar, isoscalar boson ϕ. Interest in this explanation has been stimulated by the fact that such particles (with undetermined mass) are called for in unified gauge theories of the weak and electromagnetic interactions. Letting $g_{\phi\mu\bar{\mu}}$ and $g_{\phi N\bar{N}}$ denote the ϕ-muon and the ϕ-nucleon scalar couplings, and M_ϕ the ϕ mass, the potential produced by ϕ exchange between a muon and a nucleus of nucleon number A [Fig. 4(c)] is the simple Yukawa form[27]

$$V_\phi(r) = -\frac{g_{\phi\mu\bar{\mu}}g_{\phi N\bar{N}}}{4\pi}A\frac{e^{-M_\phi r}}{r}. \quad (53)$$

Since a repulsive potential is required to remove the x-ray discrepancy, fitting Eq. (53) to the x-ray data will necessarily give $g_{\phi\mu\bar{\mu}}g_{\phi N\bar{N}} < 0$. As shown in Appendix C, this sign for the product of couplings is not possible in the simplest forms of gauge models, in which there is only one physical scalar meson and in which the chiral SU(3)⊗SU(3) symmetry-breaking term in the strong-interaction Lagrangian transforms as pure $(3,\bar{3})\oplus(\bar{3},3)$. Nonetheless, let us proceed in a purely phenomenological fashion and make a quantitative fit of Eq. (53) to the x-ray data. Replacing $\delta V(r)$ in Eq. (22) by $V_\phi(r)$, we find

$$\delta\bar{E}'_\gamma \equiv \frac{\delta\bar{E}_\gamma}{(A/2Z)} = 2.82\times 10^4 g_{\phi\mu\bar{\mu}}\, g_{\phi N\bar{N}} f_\gamma[M_\phi{}^2], \quad (54)$$

with $\delta\bar{E}'_\gamma$ the "reduced discrepancy" appropriate to a potential which couples to A rather than to Z. The experimentally measured values of $\delta\bar{E}'_\gamma$ are tabulated in Table VII. Since in all gauge models the ϕ-electron coupling is expected to be of order $(m_e/m_\mu)g_{\phi\mu\bar{\mu}}$, the ϕ will have a negligible effect on the electron $g_e - 2$ and Lamb-shift measurements. So in fitting Eq. (54) to the data we minimize $\chi^2{}_1$ defined in Eq. (48), giving the results shown in Table VIII, in good agreement with the results quoted by Sundaresan and Watson.[28]

TABLE VII. Reduced discrepancies for scalar-meson calculation.

Element $_zE$	Transition $^nl \to {}^{n-1}l - 1$	Reduced average discrepancy $-\delta\bar{E}'_\gamma$
$_{20}$Ca	$^3d \to {}^2p$	$(37.2\pm 54)\times 10^{-3}$
$_{22}$Ti	$^3d \to {}^2p$	$(11.0\pm 41)\times 10^{-3}$
$_{26}$Fe	$^3d \to {}^2p$	$(35.1\pm 30)\times 10^{-3}$
$_{38}$Sr	$^4f \to {}^3d$	$(15.5\pm 37)\times 10^{-3}$
$_{47}$Ag	$^4f \to {}^3d$	$(42.9\pm 26)\times 10^{-3}$
$_{48}$Cd	$^4f \to {}^3d$	$(17.5\pm 23)\times 10^{-3}$
$_{50}$Sn	$^4f \to {}^3d$	$(36.6\pm 22)\times 10^{-3}$
$_{56}$Ba	$^4f \to {}^3d$	$(81.0\pm 19)\times 10^{-3}$
	$^5g \to {}^4f$	$(20.0\pm 32)\times 10^{-3}$
$_{80}$Hg	$^5g \to {}^4f$	$(57.0\pm 21)\times 10^{-3}$
$_{81}$Tl	$^5g \to {}^4f$	$(43.9\pm 21)\times 10^{-3}$
$_{82}$Pb	$^5g \to {}^4f$	$(58.5\pm 17)\times 10^{-3}$

Since a light scalar boson, as well as a vacuum-polarization anomaly, can satisfactorily fit the x-ray discrepancy, let us examine ways of distinguishing between the two possible explanations. First we consider the muonic-helium Lamb shift. Since $f_{\mathrm{He}}(w) \approx \bar{f}_\gamma(w)$ for $0 \leq w \leq 6$, a scalar boson in the mass range from 1 to 22 MeV predicts an effect within about 20% of −0.027 eV, while for scalar bosons lighter than 1 MeV (corresponding to $w < 0$), the muonic-helium Lamb shift decreases as

$$\delta\mathcal{L}([^4\mathrm{He}, \mu]^+) \sim \frac{-0.178 M_\phi{}^2}{(1+0.65M_\phi)^4} \text{ eV}, \quad (55)$$

where M_ϕ is in MeV. Hence the muonic-helium experiment could only distinguish between a very light scalar boson[29] and the joint possibilities of a heavier scalar boson or a vacuum-polarization effect. On the other hand, the muonic vertex correction involving scalar-meson exchange makes a small positive[20] contribution to a_μ, as distinct from the sizable negative contribution predicted by a vacuum-polarization anomaly. So the next generation of $g_\mu - 2$ experiments should unambiguously distinguish between the vacuum-

TABLE VIII. Results of scalar-meson fits.

M_ϕ (MeV)	$\chi^2{}_1$	$(g_{\phi\mu\bar{\mu}}g_{\phi N\bar{N}})/4\pi$
0.5	8.1	-1.3×10^{-7}
1	7.9	-1.4×10^{-7}
4	6.8	-2.0×10^{-7}
8	6.1	-3.8×10^{-7}
12	6.5	-6.9×10^{-7}
16	7.5	-1.2×10^{-6}
22	10.1	-2.5×10^{-6}

polarization and scalar-meson explanations for the muonic-atom x-ray discrepancy.

ACKNOWLEDGMENTS

I wish to thank M. Baker, K. Johnson, and, above all, S. Brodsky for conversations which stimulated the muonic x-ray part of this paper. I have benefited from conversations with J. Bahcall, L. S. Brown, R. F. Dashen, B. Lautrup, B. W. Lee, J. Rafelski, V. Telegdi, S. B. Treiman, W. J. Weisberger, T.-M. Yan, and A. Zee, and wish to thank S. B. Treiman for reading the manuscript.

APPENDIX A: VECTOR-MESON PARAMETERS

For the ω and ϕ vector-meson parameters we take[30]

$$M_\omega = 784\ \text{MeV}, \quad \Gamma(\omega \to e^+e^-) = 0.76\ \text{keV},$$
$$M_\phi = 1019\ \text{MeV}, \quad \Gamma(\phi \to e^+e^-) = 1.36\ \text{keV}. \tag{A1}$$

For $F_\pi(t)$ we use the Gounaris-Sakurai formula[31] with an $\omega \to 2\pi$ interference term,[30]

$$F_\pi(t) = \frac{M_\rho{}^2(1+\delta\Gamma_\rho/M_\rho)}{M_\rho{}^2 - t + H(t) - iM_\rho\Gamma_\rho(k/k_\rho)^3 M_\rho/\sqrt{t}} + Ae^{i\alpha}\frac{M_\omega{}^2}{M_\omega{}^2 - t - iM_\omega\Gamma_\omega},$$

$$H(t) = \frac{\Gamma_\rho M_\rho{}^2}{k_\rho{}^3}\{k^2[h(t) - h(M_\rho{}^2)] + k_\rho{}^2 h'(M_\rho{}^2)(M_\rho{}^2 - t)\},$$

$$h(t) = \frac{2}{\pi}\frac{k}{\sqrt{t}}\ln\left(\frac{\sqrt{t}+2k}{2m_\pi}\right), \tag{A2}$$

$$h'(M_\rho{}^2) = \frac{1}{2\pi M_\rho{}^2} + \frac{m_\pi{}^2}{\pi M_\rho{}^3 k_\rho}\ln\left(\frac{M_\rho + 2k_\rho}{2m_\pi}\right),$$

$$k = (\tfrac{1}{4}t - m_\pi{}^2)^{1/2}, \quad k_\rho = (\tfrac{1}{4}M_\rho{}^2 - m_\pi{}^2)^{1/2},$$

$$A = \frac{6B^{1/2}(\omega \to ee)\Gamma_\omega}{\alpha M_\omega \beta_\pi{}^{3/2}} B^{1/2}(\omega \to 2\pi),$$

$$\beta_\pi = \left(1 - \frac{4m_\pi{}^2}{t}\right)^{1/2},$$

with the following values for the parameters[30]:

$$\delta = 0.6, \qquad \alpha = 86^\circ,$$
$$M_\rho = 775\ \text{MeV}, \quad \Gamma_\omega = 9.2\ \text{MeV},$$
$$\Gamma_\rho = 149\ \text{MeV}, \quad B^{1/2}(\omega \to ee) = 0.906\times10^{-2}, \tag{A3}$$
$$m_\pi = 140\ \text{MeV}, \quad B^{1/2}(\omega \to 2\pi) = 0.19.$$

As discussed in Appendix B, approximating the small-t region in this fashion as a sum of ω, ϕ, and ρ contributions should yield the small-t contribution to $T_{\text{obs}}(-s)$ (which is only a small fraction of the total for large $-s$) to an accuracy of about 15%.

APPENDIX B: FORMULAS FOR $f_a[t]$ AND THE HADRONIC CONTRIBUTION TO $g_\mu - 2$

The function $f_a[t]$ appearing in Eq. (27) has been evaluated by Brodsky and de Rafael,[32] who find

$$f_a[t] \equiv 2K(t),$$
$$0 \le t \le 4m_\mu{}^2, \quad \tau = t/4m_\mu{}^2,$$
$$K(t) = \tfrac{1}{2} - 4\tau - 4\tau(1-2\tau)\ln(4\tau) - 2(1-8\tau+8\tau^2)\left(\frac{\tau}{1-\tau}\right)^{1/2}\arctan\left(\frac{1-\tau}{\tau}\right)^{1/2};$$
$$t \ge 4m_\mu{}^2, \quad x = \frac{1-(1-4m_\mu{}^2/t)^{1/2}}{1+(1-4m_\mu{}^2/t)^{1/2}},$$
$$K(t) = \tfrac{1}{2}x^2(2-x^2) + (1+x)^2(1+x^2)\frac{\ln(1+x) - x + \frac{1}{2}x^2}{x^2} + \frac{1+x}{1-x}x^2\ln x. \tag{B1}$$

Corresponding to the division of $T_{\text{obs}}(-s)$ into four pieces in Eq. (15), we write the hadronic contribution to a_μ as

$$a_\mu = \frac{1}{4\pi^3}\int_{4m_\pi{}^2}^\infty dt\,\sigma(e^+e^- \to \text{hadrons}; t)K(t)$$
$$= a_\mu^{\omega+\phi} + a_\mu^\rho + a_\mu^{\text{cont}(1)} + a_\mu^{\text{cont}(2)}. \tag{B2}$$

Working in the same narrow-resonance approximation as in the text, we find for $a_\mu^{\omega+\phi}$ the expression[6]

$$a_\mu^{\omega+\phi} = \sum_{V=\omega,\phi}\frac{3}{\pi}K(M_V{}^2)\frac{\Gamma(V \to e^+e^-)}{M_V}, \tag{B3}$$

while a_μ^ρ is given by the integral

$$a_\mu^\rho = \frac{\alpha^2}{12\pi^2}\int_{4m_\pi{}^2}^\infty \frac{dt}{t}\left(1 - \frac{4m_\pi{}^2}{t}\right)^{3/2}|F_\pi(t)|^2 K(t). \tag{B4}$$

Substituting the parameters from Appendix A and evaluating Eqs. (B3) and (B4) numerically gives

$$a_\mu^{\omega+\phi} = 9.1\times10^{-9}, \quad a_\mu^\rho = 45\times10^{-9},$$
$$a_\mu^{\text{tot small } t} = 54\times10^{-9}. \tag{B5}$$

A more elaborate evaluation of the small-t contribution has been given by Bramôn, Etim, and Greco,[33] who sum the contributions of the various important hadronic states directly from Eq. (B2), giving

$$a_\mu^{\text{tot small } t} = (61\pm7)\times10^{-9}, \tag{B6}$$

indicating that our method of treating the small-t region is good to about 15%. To evaluate $a_\mu^{\text{cont}(1)}$

and $a_\mu^{\text{cont}(2)}$ we approximate $K(t)$ by its asymptotic form

$$K(t) \approx \tfrac{1}{3} m_\mu{}^2/t\,, \quad t \to \infty\,, \tag{B7}$$

giving [in units where unity = (1 GeV/c)^2]

$$a_\mu^{\text{cont}(1)} = 6.7\times 10^{-9} \int_{0.39}^{25} \frac{dtR(t)}{t^2}\,,$$
$$a_\mu^{\text{cont}(2)} = 6.7\times 10^{-9} \int_{25}^{t_C} \frac{dtR(t)}{t^2}\,. \tag{B8}$$

Evaluating $a_\mu^{\text{cont}(1)}$ numerically using the data plotted in Fig. 1 gives

$$a_\mu^{\text{cont}(1)} = 9.6 \pm 2\,, \tag{B9}$$

with the error a rough guess. Thus the total known hadronic contribution to a_μ is

$$(61\pm 7)\times 10^{-9} + (9.6\pm 2)\times 10^{-9} = (71\pm 7)\times 10^{-9}\,. \tag{B10}$$

Estimating the unmeasured contribution by assuming a linearly rising $R(t)$ up to $t_C = (2.230)^2$, we get

$$a_\mu^{\text{cont}(2)} = 6.7\times 10^{-9}\times 0.24\times \ln\left(\frac{(460)^2}{25}\right)$$
$$= 15\times 10^{-9}\,, \tag{B11}$$

as stated in the text.

APPENDIX C: SIGN OF THE SCALAR-MESON EXCHANGE POTENTIAL IN SIMPLE GAUGE THEORIES

Consider a gauge theory of the weak and electromagnetic interactions in which only one scalar field ϕ develops a vacuum expectation, $\phi \to \phi + \lambda$, as a result of spontaneous symmetry breaking. Since λ is the source of the lepton masses, the interaction Hamiltonian (= − the interaction Lagrangian) coupling ϕ to the muons is[34]

$$\mathcal{H}_{\phi\mu\bar{\mu}} = \frac{\phi}{\lambda} m_\mu \bar{\psi}_\mu \psi_\mu\,. \tag{C1}$$

Since in the hadronic sector λ is the origin of chiral SU(3)⊗ SU(3) symmetry breaking, the interaction Hamiltonian coupling ϕ to the hadrons is[34]

$$\mathcal{H}_{\phi\,\text{hadron}} = \frac{\phi}{\lambda}\,\delta\mathcal{H}_{\text{chiral breaking}}\,. \tag{C2}$$

Hence the sign of $g_{\phi\mu\bar{\mu}} g_{\phi N\bar{N}}$ is the same as the sign of $\langle N|\,\delta\mathcal{H}_{\text{chiral breaking}}\,|N\rangle$. Now if $\delta\mathcal{H}_{\text{chiral breaking}}$ transforms under SU(3)⊗ SU(3) as $(3,\bar{3})\oplus(\bar{3},3)$, then using the notation of Gell-Mann, Oakes, and Renner[35] we readily find that

$$\langle N|\,\delta\mathcal{H}_{\text{chiral breaking}}\,|N\rangle = \frac{3\sigma_{\pi NN}}{(\sqrt{2}+c)\sqrt{2}} + \left(c - \frac{1}{\sqrt{2}}\right)\langle N|\,u_8|N\rangle\,,$$
$$c = -\sqrt{2}\,\frac{m_K{}^2 - m_\pi{}^2}{m_K{}^2 + \frac{1}{2}m_\pi{}^2} = -1.25\,,$$
$$\langle N|\,u_8|N\rangle = \text{baryon mass splitting parameter} = 170\ \text{MeV}\,,$$
$$\sigma_{\pi NN} \equiv \tfrac{1}{3}(\sqrt{2}+c)\langle N|\,\sqrt{2}\,u_0 + u_8|N\rangle\,. \tag{C3}$$

That is, we have

$$\langle N|\,\delta\mathcal{H}_{\text{chiral breaking}}\,|N\rangle = 12.9\sigma_{\pi NN} - 333\ \text{MeV}\,. \tag{C4}$$

Recent determinations of the σ term $\sigma_{\pi NN}$ suggest a value in the range 45–85 MeV,[36] making $\langle N|\,\delta\mathcal{H}_{\text{chiral breaking}}\,|N\rangle$ positive and giving an attractive scalar-meson exchange force. A value of $\sigma_{\pi NN}$ smaller than 25 MeV would be needed to make the scalar-meson exchange force repulsive, as is required to explain the muonic x-ray discrepancy.

[1] For a summary of the recent data, see R. Gatto and G. Preparata, Phys. Lett. 50B, 479 (1974).

[2] A good review of the relevant experiments and theory is given by P. J. S. Watson and M. K. Sundaresan, Can. J. Phys. 52, 2037 (1974).

[3] L. Silvestrini, in *Proceedings of the XVI International Conference on High Energy Physics, Chicago-Batavia, Ill., 1972,* edited by J. D. Jackson and A. Roberts (NAL, Batavia, Ill., 1973), Vol. 4, p. 1.

[4] T. Appelquist and H. Georgi, Phys. Rev. D 8, 4000 (1973); A. Zee, *ibid.* 8, 4038 (1973).

[5] See, for example, C. H. Llewellyn Smith, CERN Report No. CERN TH. 1849, 1974 (unpublished); N. Cabibbo and G. Karl, CERN Report No. CERN TH. 1858, 1974 (unpublished).

[6] We follow the treatment of the vector-meson contributions to $\sigma(e^+e^- \to \text{hadrons};t)$ given by M. Gourdin and E. de Rafael, Nucl. Phys. B10, 667 (1969).

[7] J. Arafune, Phys. Rev. Lett. 32, 560 (1974); L. S. Brown, R. N. Cahn, and L. D. McLerran, *ibid.* 32, 562 (1974); M. Gyulassy, *ibid.* 32, 1393 (1974).

[8] J. Rafelski, B. Müller, G. Soff, and W. Greiner, Univ. of Pennsylvania report (unpublished).

[9] M. S. Dixit *et al.*, Phys. Rev. Lett. 27, 878 (1971).

[10] H. Walter *et al.*, Phys. Lett. 40B, 197 (1972).

[11] S. L. Adler, Phys. Rev. D 5, 3021 (1972); K. Johnson and M. Baker, *ibid.* 8, 1110 (1973).

[12] M. K. Sundaresan and P. J. S. Watson, Phys. Rev. Lett. 29, 15 (1972); L. Resnick, M. K. Sundaresan, and

P. J. S. Watson, Phys. Rev. D 8, 172 (1973).

[13]To make the definition of $\delta\rho$ precise, we are assuming $\delta\rho$ to be an extra contribution to the vacuum-polarization two-point spectral function above and beyond the usual second- and fourth-order electron and muon contributions, of a magnitude much larger than the naive perturbative estimate of the sixth- and higher-order terms. Because $Z\alpha$ is not a very small parameter for some of the atomic species being considered, in establishing the existence of the muonic anomaly it is important to take into account $4, 6, \ldots$-point vacuum-polarization amplitudes in which one vertex emits a photon coupling to the muon and all the remaining vertices couple to the nuclear Coulomb potential. Numerically, the contribution of such diagrams to the x-ray energies is only a few percent of the Uehling potential contribution, so we neglect possible nonperturbative modifications of the higher-point functions.

[14]Just to set the energy scale involved, the Uehling energies are typically 0.2–3 keV out of total transition energies of 150–500 keV.

[15]We assume independence of errors and add errros in quadrature for both the muonic discrepancies and the Lamb-shift measurements. If systematic errors are large, then the errors for average quantities will be larger than those quoted, making the constraints on the χ^2 fits less restrictive than those we have assumed.

[16]B. Lautrup, A. Petermann, and E. de Rafael, Phys. Rep. 3C, 193 (1972).

[17]V. W. Hughes, in *Atomic Physics 3,* edited by S. J. Smith and G. K. Walters (Plenum, New York, 1973), p. 1; B. Lautrup (unpublished).

[18]B. Lautrup, Phys. Lett. 38B, 408 (1972); M. A. Samuel, Phys. Rev. D 9, 2913 (1974).

[19]C. H. Llewellyn Smith, Ref. 5; N. Cabibbo and R. Gatto, Phys. Rev. 124, 1577 (1961).

[20]R. Jackiw and S. Weinberg, Phys. Rev. D 5, 2396 (1972); I. Bars and M. Yoshimura, *ibid.* 6, 374 (1972); J. R. Primack and H. R. Quinn, *ibid.* 6, 3171 (1972).

[21]The atomic fermium K_α x-ray measurements of P. F. Dittner *et al.* [Phys. Rev. Lett. 26, 103 (1971)] only probe the Uehling potential to an accuracy of about 20%. See B. Fricke *et al.*, Phys. Rev. Lett. 28, 714 (1972). Constraints imposed by timelike photon vertex measurements are discussed in S. L. Adler, R. F. Dashen, and S. B. Treiman, following paper, Phys. Rev. D 10, 3728 (1974).

[22]N. M. Kroll, in *Atomic Physics 3,* edited by S. J. Smith and G. K. Walters (Plenum, New York, 1973), p. 33.

[23]The data are taken from Ref. 16, except for Li^{++}, where we use the more accurate measurements of P. Leventhal and P. G. Havey, Phys. Rev. Lett. 32, 808 (1974).

[24]The conclusion that satisfactory fits can be found has also been reached by F. Heile (unpublished), using a momentum-space parametrization of the vacuum-polarization discrepancy.

[25]S. L. Adler, R. F. Dashen, and S. B. Treiman (in preparation). We show in this paper that a decrease in the vacuum-polarization spectral function necessarily implies a decrease in the vertex for emission of a timelike photon, and tests of the effect are suggested. Obviously, modifications in vertex parts will at some level make contributions to the electrodynamic processes discussed in the present paper above and beyond the direct effect of the postulated vacuum-polarization discrepancy. There seems at present to be no way of estimating the size of such additional contributions; about all one can say is that they are likely to be most important in the electron Lamb shift and $g_e - 2$ experiments, where only one mass scale (m_e) is involved and the vacuum-polarization and photon-electron vertex parts are off-shell to a similar degree. Hence the electronic Lamb-shift predictions of Tables V and VI should not be taken too literally. On the other hand, in the muon energy level and $g_\mu - 2$ experiments, two mass scales (both m_e and m_μ) are involved, with the electron vacuum-polarization loops much further off-shell (relative to their natural mass scale) than are the photon-muon vertices. Thus in this case the neglect of possible vertex modifications, which is implicit in all of the discussion of the text, may well be justified.

[26]E. Campini, Lett. Nuovo Cimento 4, 982 (1970); P. J. S. Watson and M. K. Sundaresan, Ref. 2. As both of these references emphasize, in order for muonic helium to be useful for electrodynamics tests, current uncertainties in the helium nuclear charge radius and nuclear polarizability will have to be reduced.

[27]The factor $(4\pi)^{-1}$ in Eq. (49) appears to have been omitted in the basic paper of R. Jackiw and S. Weinberg, Phys. Rev. D 5, 2396 (1972) and in subsequent papers quoting their formulas.

[28]Because of the factor of 4π mentioned in Ref. 26, our $(g_{\phi\mu\bar{\mu}} g_{\phi N\bar{N}})/4\pi$ should be compared with $g_{\phi\mu\bar{\mu}} g_{\phi N\bar{N}}$ of Ref. 2. Omitting the $_{20}$Ca, $_{22}$Ti, $_{26}$Fe, and $_{38}$Sr discrepancies from the fit, as was done in Ref. 2, we find an effective coupling of -7.6×10^{-7} at $M_\phi = 12$ MeV, in agreement with the magnitude of 8.0×10^{-7} quoted in Ref. 2. The numerical results of Table VIII were obtained by fitting to all discrepancy data.

[29]The possibility of a very light scalar meson may well be almost academic. An experiment reported by D. Kohler, J. A. Becker, and B. A. Watson [Phys. Rev. Lett. 33, 1628 (1974)] looks, via the e^+e^- decay mode, for a ϕ produced in the transition from ^{16}O(6.05 MeV) and ^{4}He(20.2 MeV) 0^+ states to the 0^+ ground states, and concludes that M_ϕ cannot be between 1.030 MeV and 18.2 MeV. Furthermore, neutron-electron scattering data rule out $M_\phi \lesssim 0.6$ MeV (see Ref. 24), leaving only a narrow allowed region between 0.6 and 1.03 MeV. These remarks do not apply to the derivative-coupled ϕ discussed recently by S. Barshay (unpublished), where the electron coupling is smaller than the μ coupling by two, as opposed to one, powers of m_e/m_μ.

[30]The data used are taken from J. Lefrançois, in *Proceedings of the 1971 International Symposium on Electron and Photon Interactions at High Energies,* edited by N. B. Mistry (Laboratory of Nuclear Studies, Cornell University, Ithaca, N. Y., 1972), p. 51.

[31]G. J. Gounaris and J. J. Sakurai, Phys. Rev. Lett. 21, 244 (1968).

[32]S. J. Brodsky and E. de Rafael, Phys. Rev. 168, 1620 (1968); 174, 1835 (1968).

[33]A. Bramòn, E. Etim, and M. Greco, Phys. Lett. 39B, 514 (1972).

[34]R. Jackiw and S. Weinberg, Ref. 20.

[35]M. Gell-Mann, R. J. Oakes, and B. Renner, Phys. Rev.

175, 2195 (1968). See also B. Renner, in *Springer Tracts in Modern Physics*, edited by G. Höhler and E. A. Niekisch (Springer, New York, 1972), Vol. 61, p. 121.

[36]H. Pilkuhn *et al.*, Nucl. Phys. B65, 460 (1973). See especially pp. 480–481. The estimate of Eq. (C4) is also given by E. Reya, Rev. Mod. Phys. 46, 545 (1974). Reya writes $M_B = M_0 + \langle B|\delta\mathcal{H}_{\text{chiral breaking}}|B\rangle$, where M_0 is the baryon mass in the absence of SU(3)⊗SU(3) breaking. For the $(3,\bar{3})\oplus(\bar{3},3)$ case, he finds $M_0 = 1300\ \text{MeV} - 13\sigma_{\pi NN}$, so for $\sigma_{\pi NN}$ in the range 45–85 MeV the mass M_0 is less than the nucleon mass, making $\langle N|\delta\mathcal{H}_{\text{chiral breaking}}|N\rangle$ positive.

PHYSICAL REVIEW D VOLUME 10, NUMBER 11 1 DECEMBER 1974

Comments on proposed explanations for the muonic-atom x-ray discrepancy

Stephen L. Adler and Roger F. Dashen
Fermi National Accelerator Laboratory, Batavia, Illinois 60510
and The Institute for Advanced Study, Princeton, New Jersey 08540

S. B. Treiman*
Fermi National Accelerator Laboratory, Batavia, Illinois 60510
(Received 12 August 1974)

Two proposed explanations for the apparent muonic-atom x-ray discrepancy are the possible existence of nonperturbative vacuum polarization modifications and the possible existence of a weakly coupled light scalar boson. We show that a nonperturbative decrease in the vacuum polarization spectral function implies a reduction in the vertex for a timelike photon to couple to an electron-positron pair. This would lower by a few percent the rate for π^0 Dalitz decay and suggests observable effects in the colliding beam reactions $e^+e^- \to e^-e^+$, $e^+e^- \to \mu^\pm\mu^\mp$. Turning to the scalar-boson hypothesis, we use neutron-electron and electron-deuteron scattering data to show that a scalar particle with mass lighter than about 0.6 MeV cannot be invoked to explain the muonic discrepancy. We conclude by discussing the useful role which isotope effects and pionic-atom experiments might play in determining the phenomenological structure of the extra potential implied by the discrepancy.

Recent studies of the x-ray spectra in muonic atoms have shown persistent discrepancies between theory and experiment.[1] These discrepancies, if confirmed in future measurements of higher resolution, will require modification of the usual quantum-electrodynamic theory used for calculating the muonic-atom energy levels. Phenomenologically, the required modification takes the form of an additional repulsive potential $\delta V(r)$ seen by the orbiting muon, which if written as a superposition of Yukawa potentials,

$$\delta V(r) = \int d\sigma\, w(\sigma)\frac{e^{-\sigma r}}{r}, \tag{1}$$

can involve masses σ in the range from 0 to ~22–30 MeV.[1] At a fundamental level, the potential of Eq. (1) could arise from various sources. One possible origin[2] would be the presence of nonperturbative vacuum-polarization modifications, which would change the usual vacuum-polarization potential given by the lowest two orders of perturbation theory,[3]

$$V_{\text{VP}}(r) = -Z\frac{\alpha^2}{3\pi}\int_{4m_e^2}^{\infty}\frac{dt}{t}\left[\rho_e^{(0)}(t)+\rho_\mu^{(0)}(t)+\rho_e^{(1)}(t)+\rho_\mu^{(1)}(t)+\rho_{e\mu}^{(1)}(t)\right]e^{-t^{1/2}r}/r,$$

$$Z = \text{nuclear charge},$$

$$\rho_e^{(0)}(t) = (1+2m_e^2/t)(1-4m_e^2/t)^{1/2},$$

$$\rho_e^{(1)}(t) = \cdots \tag{2}$$

to read

$$V_{\text{VP}} \to V_{\text{VP}} + \delta V,$$

$$\delta V(r) = -Z\frac{\alpha^2}{3\pi}\int_{4m_e^2}^{\infty}\frac{dt}{t}\,\delta\rho(t)\frac{e^{-t^{1/2}r}}{r}. \tag{3}$$

Here $\delta\rho(t)$ (which must be negative to produce a repulsive potential) is a nonperturbative change in the vacuum-polarization spectral function, of a magnitude much larger than one's naive estimate of the sixth- and higher-order perturbation-theory terms omitted in Eq. (2). Another possible origin would be the existence of a weakly coupled light scalar, isoscalar boson ϕ coupling both to the μ